An Epidermal Plakin that Integrates Actin and Microtubule Networks at Cellular Junctions

Iakowos Karakesisoglou, Yanmin Yang, and Elaine Fuchs

Howard Hughes Medical Institute, Department of Molecular Genetics and Cell Biology, The University of Chicago, Chicago, Illinois 60637

Abstract. Plakins are cytoskeletal linker proteins initially thought to interact exclusively with intermediate filaments (IFs), but recently were found to associate additionally with actin and microtubule networks. Here, we report on ACF7, a mammalian orthologue of the *Drosophila* kakapo plakin genetically involved in epidermal–muscle adhesion and neuromuscular junctions. While ACF7/kakapo is divergent from other plakins in its IF-binding domain, it has at least one actin (K_d = 0.35 μM) and one microtubule (K_d ~6 μM) binding domain. Similar to its fly counterpart, ACF7 is expressed in the epidermis. In well spread epidermal keratinocytes, ACF7 discontinuously decorates the cytoskeleton at the cell periphery, including microtubules (MTs) and actin filaments (AFs) that are aligned in parallel converging at focal contacts. Upon calcium induction of intercellular adhesion, ACF7 and the cytoskeleton reorganize at cell–cell borders but with different kinetics from adherens junctions and desmosomes. Treatments with cytoskeletal depolymerizing drugs reveal that ACF7's cytoskeletal association is dependent upon the microtubule network, but ACF7 also appears to stabilize actin at sites where microtubules and microfilaments meet. We posit that ACF7 may function in microtubule dynamics to facilitate actin–microtubule interactions at the cell periphery and to couple the microtubule network to cellular junctions. These attributes provide a clear explanation for the *kakapo* mutant phenotype in flies.

Key words: kakapo • ACF7 • cytoskeleton • integrins • cell adhesion

Introduction

Plakins are enormous (200–700 kD) coiled-coil dimeric proteins that include desmoplakin, bullous pemphigoid antigen (BPAG) 1,[1] plectin, periplakin, and envoplakin, and which are typified by their ability to associate with intermediate filaments (IFs) through their carboxy tail segments (for review, see Ruhrburg and Watt, 1997; Fuchs and Yang, 1999). Through defined interacting domains, plakins make cross-bridges between IFs and adhesive junctions that specifically associate with this cytoskeletal component. Thus, for example, plectin and BPAG1e (the epithelial form of BPAG1) each bind to proteins in hemidesmosomes as well as IFs (Wiche et al., 1993; Yang et al., 1996; Andra et al., 1997, 1998; Rezniczek et al., 1998; Schaapveld et al., 1998; Leung et al., 1999a), whereas desmoplakin associates with components of desmosomes in addition to IFs (Stappenbeck and Green, 1992; Kouklis et al., 1994; Smith and Fuchs, 1998; Kowalczyk et al., 1997, 1999). Periplakin and envoplakin differ in that they are expressed only in terminally differentiating epidermal cells, where they appear to cross-link desmosomes and IFs to the cornified envelope (Ruhrberg and Watt, 1997).

Plakin functions have been examined through gene knockout technology, and in some organs, particularly skin, these connector molecules seem to play structural roles that partially overlap with those of the IFs to which they connect (Guo et al., 1995; Brown et al., 1995; Andra et al., 1998; Gallicano et al., 1998). Thus, the loss of either BPAG1 or plectin severs keratin IFs from hemidesmosomes and the epithelium can no longer withstand mechanical shear forces, resulting in intraepidermal rupturing and a skin blister (Guo et al., 1995; Andra et al., 1998). In humans, this condition is known as epidermolysis bullosa simplex, most frequently caused by IF-disrupting mutations in the keratins themselves (for review see Fuchs and Cleveland, 1998). Reflective of additional expression of

Address correspondence to Elaine Fuchs, Howard Hughes Medical Institute, Department of Molecular Genetics and Cell Biology, The University of Chicago, 5841 S. Maryland Avenue, Room N314, Chicago, IL 60637. Tel.: (773) 702-1347. Fax: (773) 702-0141. E-mail: nlipak@midway.uchicago.edu

[1] *Abbreviations used in this paper:* ABD, actin binding domain; AF, actin filament; BPAG, bullous pemphigoid antigen; IFs, intermediate filaments; MTs, microtubules.

the *BPAG1* gene in sensory neurons, mice defective in the *BPAG1* gene exhibit axonal swellings packed with disorganized IFs and accompanied by gross neuronal degeneration (Brown et al., 1995; Guo et al., 1995). Similarly, humans defective in the *plectin* gene display signs of muscular dystrophy, reflective of plectin's additional expression in muscle (Andra et al., 1998 and references therein). These findings underscore the importance of plakins in cell integrity and in maintaining IF cytoarchitecture.

Most plakin genes encode multiple isoforms that are differentially expressed in a tissue-specific manner (Brown et al., 1995; Bernier et al., 1996; Elliott et al., 1997). An interesting feature of plakins is that the isoforms perform functions uniquely tailored to suit the cytoskeletal needs of each specialized cell (Yang et al., 1996, 1999). Some isoforms are not limited to interconnections with IFs, but can also associate with the other cytoskeletal networks (Svitkina et al., 1996; Yang et al., 1996, 1999; Andra et al., 1998). Two neuronal forms of BPAG1 have the capacity to bind simultaneously to actin and neuronal IF networks, perhaps anchoring the neuronal IF cytoskeleton to the cortical actin microfilaments lining the axon (Yang et al., 1996; Leung et al., 1999a). Plectin also associates with actin and IF networks, but in this case, it may function in actin dynamics, as cultured plectin null fibroblasts display perturbations in cell motility and Rho/Rac/Cdc42-mediated actin rearrangements (Andra et al., 1998).

Some plakins have the capacity to bridge IFs and MTs, as was first visualized by immunoelectron microscopy of cultured fibroblasts whose actin cytoskeleton had been disrupted and extracted (Svitkina et al., 1996). An MT binding site has now been identified in BPAG1n3, a novel neural isoform that appears to function by stabilizing the network to facilitate axonal transport over long distances (Yang et al., 1999; see also Dalpe et al., 1998). An extraordinary feature of this plakin is that when NFs are removed from sensory neurons through gene targeting, BPAG1n3 still associates with MTs, classifying this protein as a bona fide MT-associated protein, or MAP (Yang et al., 1999).

Underscoring the dispensability of IFs for some plakins is the recent finding that plakins exist in lower eukaryotes such as *Drosophila*, which are devoid of IF cytoplasmic networks (Gregory and Brown, 1998; Prokop et al., 1998; Strumpf and Volk, 1998). Mutations in the insect plakin, kakapo, cause defects in neuromuscular junctions and in adhesion between epidermal and muscle cells. In flies, these processes are dependent upon interactions between integrins, MTs, and the actin cytoskeleton. While mammalian integrins are known to connect to actin microfilaments ($\alpha\beta1$) and IFs ($\alpha6\beta4$), recent evidence also suggests that MTs may be involved (Kaverina et al., 1998). Given this potential relation between mammalian and invertebrate integrin–cytoskeletal connections, it seems possible that a functional equivalent of kakapo might exist in mammals.

ACF7 is a broadly expressed mammalian plakin originally cloned on the basis of its sequence similarity to dystrophin, another linker protein bridging cytoskeleton and membrane-associated junctions (for review see Straub and Campbell, 1997). Until recently, only 6 kb of the 5′ ends of three different 14–18-kb ACF7 transcripts had been sequenced, but this was sufficient to classify it as a plakin (Byers et al., 1995; Bernier et al., 1996). Using degenerative PCR, we isolated a 3′ coding sequence from mouse ACF7 cDNA, and discovered that it was similar to *Drosophila* kakapo and identical to the recently reported full-length mouse cDNA encoding isoform 2 of ACF7 (Nagase et al., 1998; Leung et al., 1999b; Okuda et al., 1999), further illuminating the similarities between fly and mammalian sequences.

Despite such an interesting phenotype in flies, little is known about the function and/or biology of kakapo or ACF7. We were intrigued by the possibility that yet another plakin might be expressed in mammalian epidermis, given that keratinocytes are already rich with these proteins. In this study, we show that ACF7 is indeed expressed in the epidermis of mice as it is in flies, and we identify functional binding sites for both actin and MTs in ACF7/kakapo's amino-terminal segment. We show that in keratinocytes, ACF7 associates preferentially with MTs and selectively decorates those MTs that align with AFs, reside near the cell periphery, and associate with integrin-mediated focal adhesions. Upon calcium induction of intercellular adhesion, ACF7 reorganizes to align parallel to cell–cell borders in a fashion that mimics, but is not dependent upon, MTs. Our findings provide major new insights into the biology of this relatively little explored plakin, and directly implicate this cytoskeletal linker protein in cellular adhesion. Based upon its localization, dynamics, and biochemistry, we posit that ACF7/kakapo may function specifically at sites where actin and MT cytoskeletons interface and integrate with cellular junctions.

Materials and Methods

Isolation of Mouse ACF7 cDNAs and Generation of ACF7 Antibodies

Oligonucleotide primers to ACF7 expressed sequence tag and cDNA sequences in databases were used to perform reverse transcriptase–PCR on keratinocyte and brain mRNAs. PFU TurboDNA polymerase (Stratagene) was used for high fidelity transcription. PCR fragments were cloned into the pGEX-2TK plasmid (Pharmacia). Cloned cDNAs were sequenced using the dideoxy-chain termination method (Sequenase Version 2; USB).

GST fusion proteins were engineered to contain in-frame the sequence encompassing amino acids 1,622–1,817 of ACF7 isoform 1, corresponding to the amino-terminal end of the putative coiled-coil rod segment (Bernier et al., 1996). ACF7 sequences were inserted into the EcoRI site of pGEX-2TK (Pharmacia), encoding the bacterial GST protein. Proteins were purified in two steps using (1) binding to GST-conjugated Sepharose beads, and (2) FPLC anion affinity chromatography of bound protein (Kouklis et al., 1994). Preimmune sera were screened against cross-reactivity with mouse skin extracts, and rabbit polyclonal antibodies were generated by Cocalico Biologicals, Inc. (animals were injected with 250 μg fusion protein, followed by boosts of 150 μg protein). In addition, a peptide corresponding to amino acids 178–200 of the putative actin binding domain of the ACF7 isoform 1 was synthesized, and rabbit polyclonal antisera were made by Zymed Laboratories, Inc. All antibodies were purified by affinity chromatography.

Construction of pACF7m1-HA and pACF7abd-HA and Transfections

Mouse sequences encoding the 885 amino acid encompassing the M1 segment (amino acids 212–1,097 of ACF7 isoform 1), or the 228 amino acid encompassing the ABD segment (amino acids 17–245 of ACF7 isoform 1) were subcloned in-frame at the EcoRI and NotI restriction endonuclease sites of pMH, a mammalian expression vector containing the CMV major

early promoter and enhancer. ACF7 sequences were inserted in-frame 5′ to the 9–amino acid HA epitope tag, followed by a 3′ UTR and polyadenylation site all within the vector. These constructs, pACF7m1-HA and pACF7abd-HA, were used for transient transfection assays (Yang et al., 1996).

SW13 human adrenal carcinoma cells were transiently transfected, and 28 h later, cells were fixed and subjected to double immunofluorescence as described previously (Yang et al., 1996).

Immunohistochemistry and Immunofluorescence Microscopy

Frozen sections (10 μm) of mouse skin were subjected to alkaline phosphatase enhanced immunohistochemistry as described by the manufacturer (Vectastain ABC-AP kit; Vector Laboratories). Antibodies used at 1:100 dilution were the following: αABD, against the putative actin binding domain of ACF7, and αRod against the rod domain of ACF7 (anti-ACF7 unless otherwise stated).

Cells were fixed with either methanol (−20°C) for 10 min, 1% glutaraldehyde, or 3.5% formaldehyde for 15 min at room temperature, and washed 3× with PBS. Cells were preblocked with 1% BSA, 0.1% Triton X-100, and 0.1% gelatin in PBS, and incubated with primary antibodies in fresh solution, at room temperature for 1–2 h. The following antibodies were used: rat anti-HA monoclonal, 1:100 of a 200 μg/ml stock (Boehringer-Mannheim), affinity-purified rabbit anti-ACF7 polyclonal (1:300), mouse monoclonal anti–α-tubulin (1:100; Amersham Life Sciences), mouse monoclonal anti–α-actin (1:500; Sigma Chemical Co.); rabbit polyclonal antidesmoplakin (1:500; Kouklis et al., 1994); mouse monoclonal anti–E-cadherin (1:500; Sigma Chemical Co.). After washing 3×, cells were incubated with secondary antibodies (1:1000, Alexa green and red), washed, mounted, and examined using immunofluorescence microscopy.

In Vitro Actin and Binding Assays

Binding assays were conducted essentially as described by Jongstra-Bilen et al. (1992). In brief, proteins in G-actin buffer (2 mM Tris, pH 8.0, 0.2 mM $CaCl_2$, 0.2 mM ATP, 0.5 mM DTT, and 0.01% sodium azide) were subjected to precentrifugation in a Beckman Airfuge to remove any aggregates. Proteins (0.1–0.4 μM) were combined with G-actin (Cytoskeleton, Inc.), and polymerization of actin was induced by adding KCl to 50 mM and $MgCl_2$ to 2 mM. After incubation for 1 h at room temperature, samples were again subjected to centrifugation (100,000 *g* for 60 min) to pellet the F-actin and its associated proteins. Fractions were separated by electrophoresis through 8.5% SDS–polyacrylamide gels, which were stained with Coomassie blue to visualize protein. The amounts of protein in the supernatant (S) or actin-containing pellet (P) were determined by densitometric scanning.

For binding assays, the M1 domain of mouse ACF7 was fused in-frame to GST in a bacterial expression vector (see Yang et al., 1996 for method). Bacterially expressed protein was purified using GST-conjugated Sepharose beads, followed by FPLC chromatography (Kouklis et al., 1994). Just before each binding assay, purified M1 domain was centrifuged at 100,000 *g* for 15 min to remove any aggregated protein. Purified bovine brain protein (Sigma Chemical Co.) was reconstituted according to the manufacturer's instructions, and tubulin polymerization experiments were carried out as previously described (Yang et al., 1999). The dissociation constant was estimated by plotting the data as a ratio of bound/free ACF7 domain versus bound ACF7 domain/MTs. Experiments were conducted in duplicate, and values differed by <10%.

Results

The Key Putative Structural Features of ACF7 and Its Expression in Mammalian Epidermis

The previous study by Bernier et al. (1996) reported an ~15-kb transcript in the brain, spinal cord, and skin, an ~14-kb transcript in the skeletal muscle and heart, and at least three different transcripts in the lungs, ranging from 14 to 18 kb. These authors also identified three ACF7 isoforms that differ in the amino-terminal sequence. Using degenerative PCR and reverse transcribed neuronal mRNA, we identified ACF7 as a highly related cousin, if not the mouse homologue, of *Drosophila* kakapo. The complete sequences of isoform 2 of mouse and human ACF7, as reported in GenBank accession number AF150755 (Leung et al., 1999b) and AB029290 (Okuda et al., 1999; Sun et al., 1999), most strongly establish this relationship. The 3′ partial cDNA sequence we isolated was identical to that reported by Leung et al. (1999b).

Fig. 1 provides the salient features predicted by computer analyses of mouse ACF7, kakapo, and BPAG1n3 sequences, which encode isoforms of 5,270–5,535, 5,497, and 2,870 amino acids, respectively. ACF7/kakapo isoforms contain two features distinguishing them from the other plakins: (1) the 3,000–4,000-amino acid central domain, which has similarities to the spectrinlike repeats of dystrophin and to the coiled-coil rod segment of plakins necessary for oligomerization (Ervasti and Campbell, 1991); and (2) the ~500 residue tail, which harbors sequence homology to the EF-hand calcium binding domain of dystrophin (Kawasaki and Kretsinger, 1995; for review see Ikura, 1996) as well as to Gas2, a protein selectively expressed in growth-arrested cells (Schneider et al., 1988) and associated with the actin filament network (Brancolini and Schneider, 1994). In addition, the majority of the head segment, including the 215 residue putative actin binding domain (ABD) of isoforms 1 and 2 and the 1,184 residue midsegments (M1 and M2) of all three ACF7 isoforms, are similar in sequence to plectin and BPAG1 neural isoforms (Bernier et al., 1996; Gregory and Brown, 1998; Strumpf and Volk, 1998). Isoform 3 of ACF7 (Bernier et al., 1996) is similar to BPAG1n3 (Yang et al., 1999) in that it is distinguished by the absence of the amino-terminal half of the ABD.

Given the sequence similarities between ACF7 and kakapo, and kakapo's involvement in epidermal–muscle adhesion in flies (Gregory and Brown, 1998), we began our investigation by exploring whether ACF7 mRNAs are expressed in epidermal keratinocytes either before or after intercellular adhesion was induced by switching to high calcium medium. Northern blot analyses revealed hybridizing transcripts of >14 kb at comparable levels before

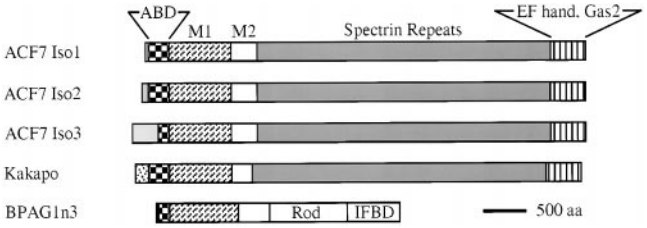

Figure 1. Stick diagram of mouse ACF7 isoforms relative to Kakapo and BPAG1n3. Bar represents 500 amino acids. ABD is split into calponin homology CH1 and CH2 segments. CH1 is missing in isoform 3 of both ACF7 and BPAG1n. The kakapo/ACF7/spectrin repeats are similar to those of dystrophin (Koenig and Kunkel, 1990; Strumpf and Volk, 1998; Okuda et al., 1999). The similarity to calcium binding EF-hand repeats are noted, as is the Gas2 homology domain (Gregory and Brown, 1998; Strumpf and Volk, 1998; Okuda et al., 1999). Other regions are shaded to denote unique sequences. IFBD, intermediate filament binding domain and Rod, coiled-coil rod segments; segments common to most plakins.

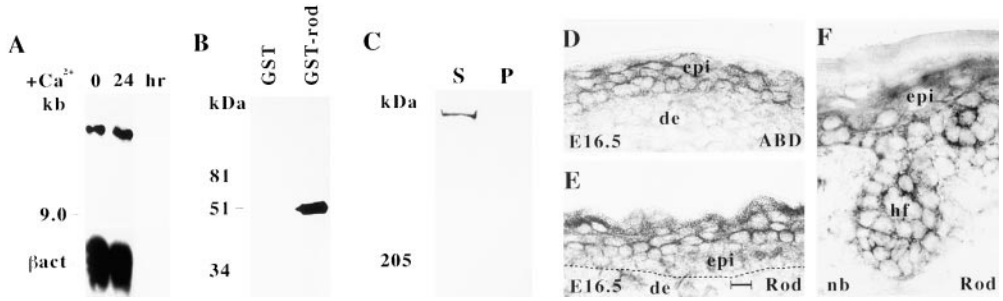

Figure 2. Conservation of epidermal expression of ACF7 from flies to mice. (A) mRNAs were isolated from primary mouse keratinocytes cultured in low calcium (0.05 mM) medium and switched to high calcium (1.5 mM) medium for 0 or 24 h. RNAs (2 μg per lane) were resolved by formaldehyde gel electrophoresis (Yang et al., 1996), and Northern blots were hybridized with radiolabeled probes against a 588-bp mouse ACF7 cDNA unique to the spectrin repeat segment common to all known isoforms (nucleotide residues 4,865–5,453 of isoform 1), or a 2-kb mouse β-actin cDNA as control. Migration of the RNA standard is indicated at left. (B) Immunoblot analysis of GST and GST ACF7 fusion proteins verified the specificity of the rod segment ACF7 antibody. (C) Anti-ACF7 immunoblot analysis of mouse epidermal keratinocyte proteins, either soluble (S) or insoluble (P) after extraction (20 mM Tris-HCl, pH 7.5, 1% Triton X-100, 1% NP-40, 1 mM PMSF, and 5 mM EDTA) and centrifugation at 10,000 *g*. Proteins were resolved by 6% SDS-PAGE and blotted (Yang et al., 1996), and after staining with Ponceau red to verify equivalent loadings, immunoblot analysis was performed with a 1:1,000 dilution of anti-ACF7. Primary antibody was followed by HRP secondary antibody and chemiluminescence (ECL method; Amersham Corp.). Migration of the muscle myosin (205 kD) control is shown. (D) Anti-ACF7 immunohistochemistry was performed on frozen 10-μm mouse skin sections from embryonic day 16.5 (E16.5) and newborn (nb). Antibodies used were either against the actin binding domain (ABD) found in isoforms 1 and 2 or the rod (Rod) domain common to the three known isoforms. Abbreviations: epi, epidermis; de, dermis; hf, hair follicle. Bar, 30 μm.

and after the calcium switch (Fig. 2 A). These findings suggested that the ~14-kb ACF7 mRNA, detected previously in whole skin (Bernier et al., 1996), stemmed at least, in part, from epidermal keratinocytes.

To examine the ACF7 protein, we raised an antibody to a coiled-coil rod segment contained within all known isoforms. As shown in Fig. 2 B, the purified antibody recognized the ACF7 rod portion of the fusion protein. In addition, this antibody recognized a single band of enormous size (>400 kD) in the soluble fraction of keratinocyte proteins extracted in nonionic detergent buffer (Fig. 2 C). This was consistent with the putative size of ACF7 isoforms (~600 kD), but illustrated a difference in solubilities of plectin and ACF7 (see Seifert et al., 1992 for comparison).

As shown in Fig. 2, D–F, ACF7 was detected in living layers of embryonic and newborn epidermis, as well as in developing hair follicles. Staining was strongest in epidermal keratinocytes, although weak staining was also observed in the dermis, which is consistent with the relatively broad distribution of ACF7 mRNAs (Bernier et al., 1996; Leung et al., 1999b; Sun et al., 1999). The specificity of ACF7 staining patterns was confirmed with two different antibodies. These data extend our in vitro findings and indicate that ACF7 is expressed in both mitotically active and differentiating keratinocytes of skin. Given the severe phenotype of the *kakapo* mutation in fly epidermis (Gregory and Brown, 1998), and the prominence of plakins in epidermal keratinocytes (for review see Ruhrberg and Watt, 1997; Fuchs and Yang, 1999), we focused the remainder of our study on exploring potential functions of ACF7 in the keratinocyte.

ACF7 Contains a Functional Actin Binding Domain

The putative ABD in the amino-terminal portion of two ACF7 isoforms suggested that ACF7 can bind AFs in a fashion similar to that of BPAG1n1/n2 and plectin (Yang et al., 1996; Andra et al., 1998). Therefore, we combined polymerized actin with the GST-ACF7 fusion protein containing this domain. As a control, we used recombinant α-actinin, containing a bona fide ABD (Fig. 3 A). In the absence of polymerized actin, both actin binding proteins were in the supernatant fraction after centrifugation at 100,000 *g*. Addition of polymerized actin resulted in a major portion of each ABD pelleting with F-actin. That these associations were specific to ABD-containing proteins was underscored by the failure of BSA or GST alone to shift to the pelletable fraction in this assay (Jongstra-Bilen et al., 1992; Lo et al., 1994; Yang et al., 1996). Note that the relative percentage of actin remaining in solution was constant, irrespective of whether an ABD was added to the polymerized preparation. This presumably was reflective of unpolymerized actin.

As the concentration of ACF7 increased, ACF7's association with polymerized actin became saturating, and soluble ACF7 levels increased. A Scatchard plot of these data revealed a dissociation constant of 0.35 μM, which was within the range of that observed for β-spectrin and other proteins with ABDs (Fig. 3 B; Jongstra-Bilen et al., 1992; Lo et al., 1994; Yang et al., 1996; Andra et al., 1998). That ACF7's ABD can associate with actin cytoskeletons in vivo was verified by using DNA transfection to express an HA-epitope–tagged ABD of ACF7 in the SW13 cell line, which lacks a cytoplasmic IF network. HA-specific antibodies and anti–β-actin colocalized with stress fibers and cortical cytoskeleton (C and D). Collectively, these data indicate that ACF7 is a bona fide actin binding protein.

ACF7 Contains a Functional MT-binding Domain

Recently, it was shown that the M1 domain of the BPAG1n3 plakin binds to MTs in vitro with a dissociation constant of 1.3 μM (Yang et al., 1999). Since this domain shares 51% sequence identity and 70% homology with the M1 domain of ACF7, we examined whether ACF7's M1 segment might also have the capacity to bind directly to MTs. In vitro binding assays were performed by combin-

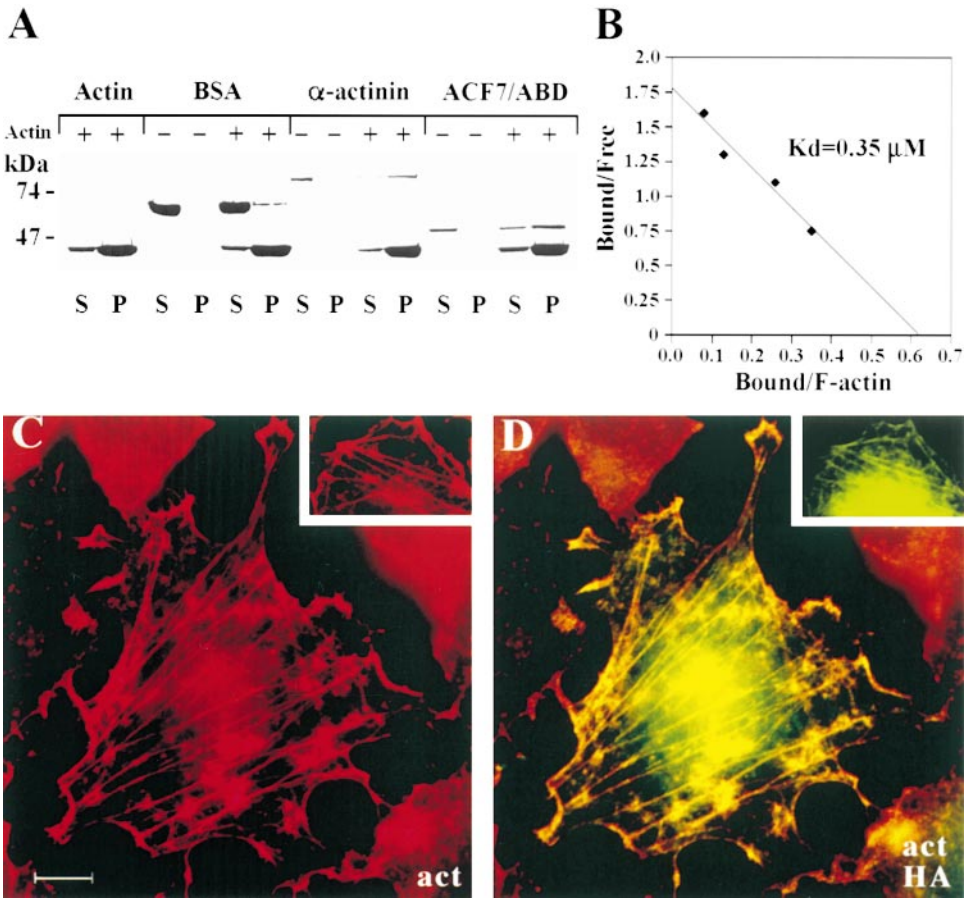

Figure 3. The putative ABD in the amino-terminal domain of ACF7 binds to AFs in vitro and colocalizes with actin networks in transfected cells. (A) Actin binding assays. Bacterial expression plasmid pGEX-2TK, containing a GST bacterial promoter (pTac) was used to produce a GST fusion protein containing amino acid residues 17–245 of isoform 1 of mouse ACF7 (ABD). After purification with GST agarose beads, AF binding assays were performed. Mouse α-actinin (Cytoskeleton, Inc.) and BSA were used as positive and negative controls, respectively. Shown is a Coomassie blue–stained gel containing aliquots of each binding assay performed with (+) and without (−) polymerized AFs and after centrifugation to separate the supernatant (S) and pellet (P) fractions. (B) Estimation of the dissociation constant of actin binding. AF binding assays were carried out as in A, except that a range of concentrations of ACF7 ABD protein was used. Scatchard plot represents an average of two data sets, with the following parameters: vertical axis, ACF7 bound/free ACF7 μM^{-1}; horizontal axis, bound ACF7/F-actin. (Calculated dissociation constant for two independent data sets differed by <10%.) (C and D) Cultured SW13 cells, lacking a cytoplasmic IF network, were transfected with pACF7abd-HA and, 48 h later, cells were costained with antibodies against the HA-epitope (green) and act, against actin (red). Shown is a transfected cell colocalizing ACF7's ABD with actin stress fibers and the cortical actin cytoskeleton. A higher magnification of ABD-decorated stress fibers is shown in a second example in C and D (insets). Bar, 10 μm.

ing purified bovine brain MTs with GST-M1 fusion protein encompassing ACF7's M1 domain. In the absence of MTs, the ACF7 fusion protein remained in the supernatant after centrifugation at 100,000 *g* (Fig. 4 A). In contrast, after addition of MTs, a portion of the ACF7 M1 protein now pelleted with them.

At higher concentrations, ACF7's association with MTs became saturating, increasing soluble ACF7 levels. A dissociation constant of ~6 μM was obtained for ACF7 binding to MTs. This dissociation constant was comparable to that of MAP-2 (1–25 μM; Wallis et al., 1993; Coffey and Purich, 1995), a well established binding protein, although the interaction was not as strong as that observed for the M1 domain of BPAG1n3 (Yang et al., 1999). A recent report suggests that an additional MT binding domain exists in the ACF7 tail segment (Leung et al., 1999b). Thus, the full-length ACF7 may have a greater affinity for MTs than this value may suggest.

To assess whether ACF7's M1 domain localizes specifically to MTs in keratinocytes, we constructed an expression vector that encoded the M1 domain of ACF7, epitope-tagged with HA. Immunoblot analysis confirmed that the transiently expressed protein was the expected size (not shown). As judged by immunofluorescence microscopy of transfected cells, the M1 domain of ACF7 gave a striking pattern of anti-HA immunofluorescence: in SW13 cells that lack an IF network, >90% of the network was decorated (Fig. 4, B–D). All three ACF7 isoforms possess the M1 domain. Whether this domain is operative in all isoforms awaits further investigation with isoform-specific antibodies.

In Epidermal Keratinocytes, ACF7 Colocalizes with Peripheral MTs

When cultured mouse keratinocytes were subjected to anti-ACF7 immunofluorescence microscopy, a striking and unusual pattern of antibody labeling was seen that was specific for the primary antibody and was not seen in preimmune sera cross-reactivity nor in controls where anti-ACF7 was omitted from the processing (Fig. 5). The majority of labeling was filamentous, and extended to cell borders (A). Double immunofluorescence with antitubulin suggested that the ACF7 colocalized with MTs (B and

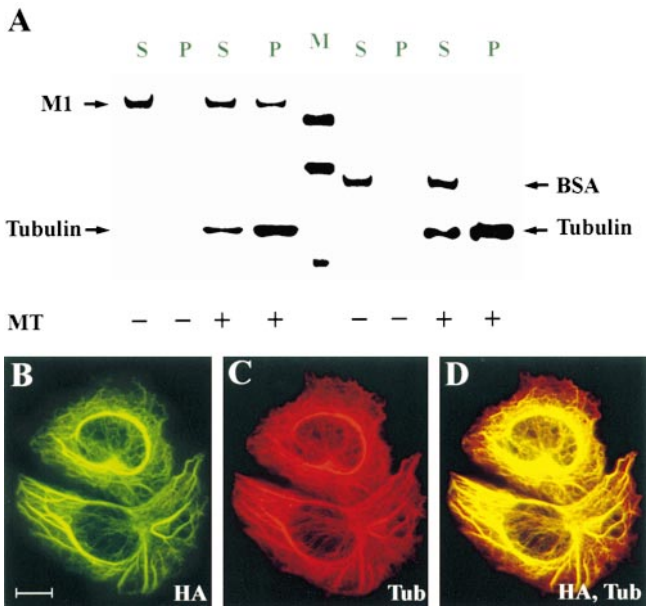

Figure 4. ACF7's M1 domain decorates MTs in transfected cells, and binds directly to MTs in vitro. (A) Binding assays were performed using the purified M1 domain of ACF7 or BSA (control) and polymerized MTs purified to >90% homogeneity from the bovine brain. After incubation, samples were subjected to centrifugation to pellet MTs and associated proteins. Fractions were separated by electrophoresis through 10% SDS–polyacrylamide gels, which were stained with Coomassie blue to visualize protein. The amounts of protein in supernatant (S) or pellet (P) were determined by densitometric scanning. Each assay was performed with (+) or without (−) polymerized MTs (MT). M, molecular mass standards (112, 84, and 53 kD). (B–D) SW13 IF-less cells were transfected with pACF7-M1-HA, expressing epitope-tagged M1 domain from ACF7. Transfected cells were fixed and subjected to immunofluorescence: mouse anti-HA (HA, green), and rabbit antitubulin (tub, red). Note that, in SW13 cells, bundling of the network occurs upon association with ACF7, a process also seen upon transient expression of other MT-associated proteins including MAP1b (Togel et al., 1998) and the M1 domain of BPAG1n3 (Yang et al., 1999). Bar, 10 μm.

C). This was true, even when the network was partially collapsed, enabling clearer visualization of individual MTs (example shown).

The patterns of anti-ACF7 labeling on MTs varied considerably within the keratinocyte population. Often, anti-ACF7 labeling was punctate and discontinuous (D and E). In the majority of cells, anti-ACF7 was more concentrated on the segments of MTs at the cell periphery than on those located more centrally within the cell (F). This was most apparent in double labelings, where antitubulin was brighter in the center of the cell and anti-ACF7 was brighter at the periphery. This intensity difference was seen with different primary antibodies and also when the fluors of secondary antibodies were switched (compare C with F). Thus, the difference appeared to be reflective of a preferential concentration of ACF7 at plus or growing ends of MTs.

The discontinuous labeling of MTs and the concentration of labeling at tips of MTs was somewhat reminiscent of the staining seen with an antibody against CLIP170, which is a protein that treadmills on plus ends of MTs and has been hypothesized to play a role in transferring cargo from MT to actin cytoskeletons (Perez et al., 1999). Since the only antibody against CLIP170 is species-specific, we examined the possibility that CLIP170 and ACF7 might colocalize in human keratinocytes. As shown in Fig. 6, A and B, the patterns were clearly distinct. Of possible importance, however, was that a number of MTs were decorated with antibodies against both proteins (arrows).

In some cells, anti-ACF7 exhibited a tuftlike appearance at the stretched borders of spread cells (Fig. 6, D–F). This labeling resembled that seen with antibodies against proteins of focal adhesions, sites where αβ1 integrin clusters make contact with cell–substratum. This was most easily seen in the double label images (F). ACF7's labeling at the cell periphery aligned with, but also extended beyond that of peripheral MTs. Most striking was ACF7's selective labeling of the cell borders (D–F, arrows). Additionally, ACF7 antibodies stained some peripheral filaments that did not appear to be MTs. We provide evidence later to suggest that these may be actin fibers, which is consistent with the bona fide ABD in some ACF7 isoforms.

To explore the possible relation between focal contacts and ACF7 in more detail, we colabeled spread cells with antibodies against ACF7 and vinculin, a focal contact protein. As shown in Fig. 6 (G–I), the anti-ACF7 pattern overlapped considerably with, but was broader than, the antivinculin pattern. The most notable difference was that filamentous staining of ACF7 at focal contacts was more extended and included more fibers than the short fibrous staining of vinculin. These results suggested that ACF7 was not a part of focal adhesions per se, but rather localized to the cytoskeleton that specifically associated with these contacts. A part, but not all, of this cytoskeleton included MTs.

ACF7 Shows a Partial Coalignment with the Actin Cytoskeleton, Particularly at Focal Contacts and Other Sites Where MTs and AFs Associate

The presence of an ABD and the preferential labeling of a focal contact–associated cytoskeleton led us to wonder whether ACF7 might also associate with the actin cytoskeleton. Double immunofluorescence labeling with antibodies against actin and ACF7 showed distinct patterns in keratinocytes (Fig. 7, A and B). While anti-actin stained cortical cytoskeleton and thin actin-rich filopodial extensions, these structures did not exhibit appreciable anti-ACF7 staining (B). However, anti-ACF7–labeled filaments often aligned with radial AFs, and some colabeled with anti-ACF7 and anti-actin antibodies (B, insets). Even more striking were occasional keratinocytes rich with actin stress fibers that colabeled with anti-ACF7 (C). Thus, while ACF7 patterns most often aligned with cytoskeletons, a few were more similar to the actin cytoskeleton. In many keratinocytes, anti-ACF7 labeling could be found in regions of the cytoskeleton where MTs and actin filaments intersect. This fraction included cytoskeleton associated with focal adhesions.

To assess whether ACF7's association with the cytoskeleton might be affected by disrupting the actin cytoskeleton, we treated keratinocytes either with 1 μg/ml latruncu-

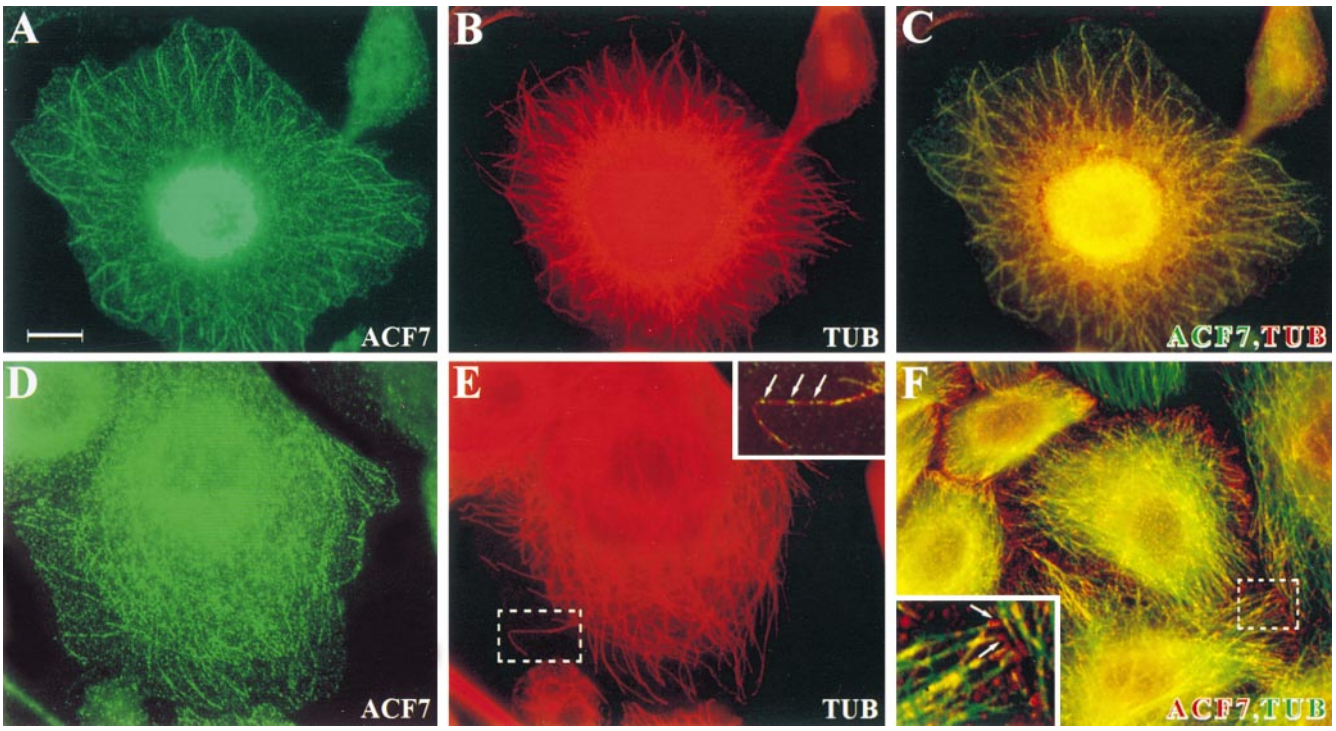

Figure 5. In epidermal keratinocytes, mouse ACF7 localizes to the network and concentrates at the tips. Mouse keratinocytes were cultured on coverslips in low calcium medium. After washing 2× in 0.1% Triton X-100, 1% BSA, and 0.1% gelatin, cells were subjected to immunofluorescence using ACF7 and tubulin antibodies as indicated in the lower right of each frame. First antibody listed is in green; the second is in red. Cell in A–C is the same; cell in D and E is the same. Insets are higher magnifications of areas in dotted white boxes. Arrows denote punctate anti-ACF7 labeling of MTs often at their tips. Bar, 10 μm.

lin B or with 10 μM cytochalasin D. The results obtained with these actin-disrupting agents were similar and, hence, we show only the data for latrunculin B. Filamentous anti-actin staining was completely abolished by 60–90 min, and dramatically diminished to punctate structures by 30 min. Under conditions where the actin cytoskeleton was completely disrupted, filamentous anti-ACF7 labeling persisted (Fig. 7). Most interesting was the staining pattern at early times after treatment, where ACF7-decorated fibers appeared to terminate at dots of anti-actin (D–F, denoted by arrowheads in F inset). Similar labeling was seen with phalloidin, indicating that the dots contained polymerized actin, and perhaps represented collapsed actin fibers. Anti–ACF7-labeled fibers appeared to be MTs as judged by costaining with antitubulin (G–I). As before, anti-ACF7 labeling was discontinuous, decorating what appeared to be distal or plus ends of MTs (I, inset).

Taken together, these data suggest that AFs may interact with the ends of a subset of MTs that are decorated with ACF7. Moreover, this interaction appears to render the MT-ACF7–associated actin more resistant to latrunculin B. Longer incubations with latrunculin B resulted in perturbations of the network and ACF7 (not shown), providing further evidence that, in some way, MTs that are decorated with ACF7 interact with actin cytoskeleton.

In contrast to other epidermal plakins, ACF7 patterns appeared to be most distinct from those of the IF cytoskeleton (Fig. 7, J–L). In the absence of IF-depolymerizing agents, we were unable to unequivocally assess whether ACF7 might associate in some localized fashion with the keratin cytoskeleton. At present, this seems unlikely given the high degree of sequence divergence between the carboxy-terminal tail of ACF7 and the characterized IF-binding domain in the tail segment of other plakins (Stappenbeck et al., 1992; Wiche et al., 1993; Kouklis et al., 1994; Kowalczyk et al., 1997). This said, the directionality of the IF cytoskeleton showed some similarities to the orientation of those MTs that were specifically labeled with ACF7.

MT-depolymerizing Agents Abolish the Filamentous Staining Pattern of Anti-ACF7

Treatment of keratinocytes with 1 μM colchicine for 30 min dramatically impaired the MT network that was abolished by 60 min. Concomitantly, filamentous anti-ACF7 staining was lost (Fig. 8, A–C). At 30 min, a few residual filamentous structures could still be seen, and these labeled both with antitubulin and anti-ACF7 (D–F). Under these conditions, the actin cytoskeleton was not noticeably perturbed (not shown). When taken together with our data on actin depolymerizing agents, these findings suggest that ACF7's association with the keratinocyte cytoskeleton depends primarily upon the integrity of the MT and not the actin network.

Interestingly, when 10 μM taxol was used for 30 min to stabilize MTs, anti-ACF7 staining still coincided with antitubulin staining (Fig. 8, G and H). The approximate

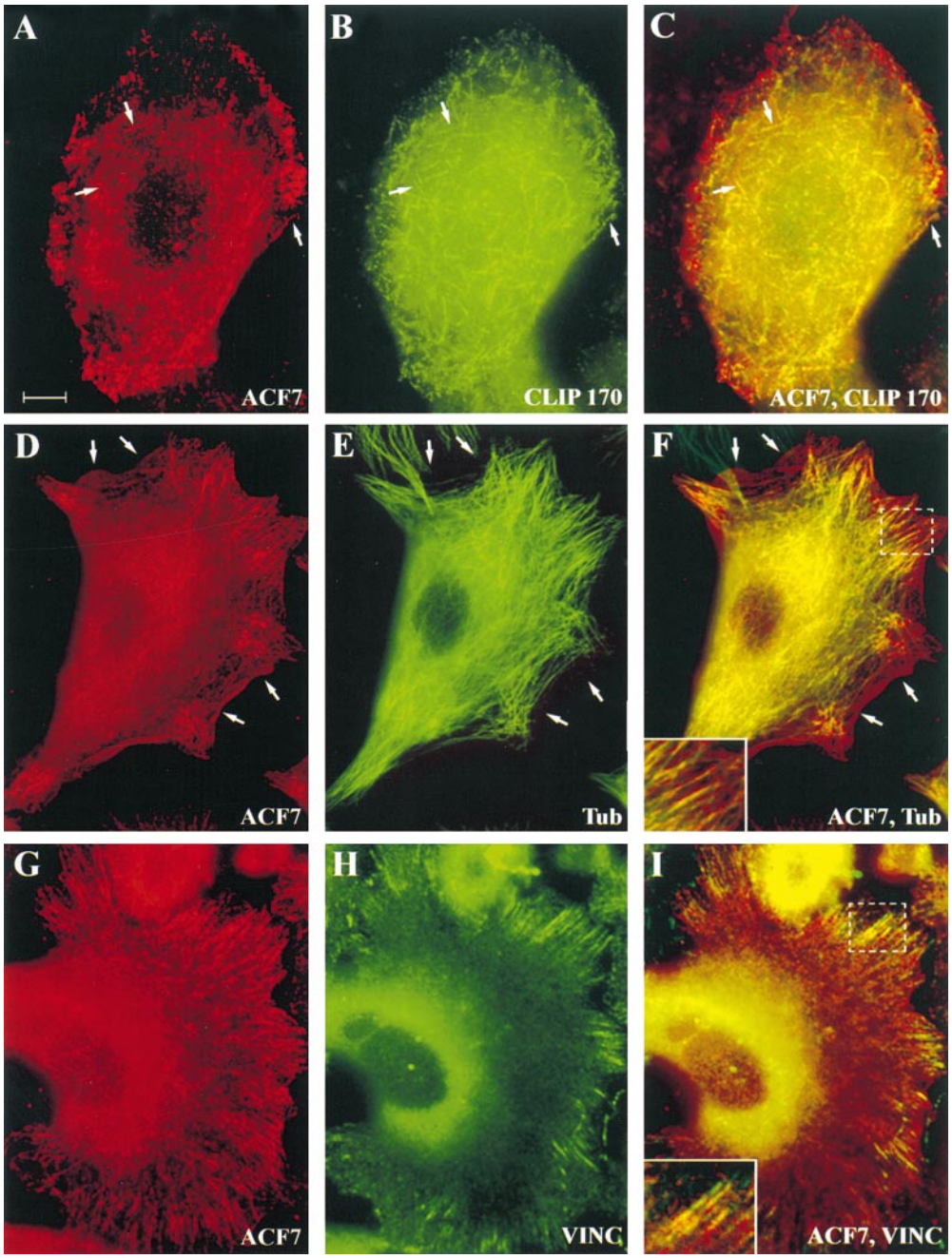

Figure 6. The distribution of mouse ACF7 shares similarities as well as differences with plus end–directed MT-treadmilling proteins and with focal adhesion structures. Keratinocytes were cultured in low calcium medium and processed for immunofluorescence microscopy. Antibodies used are indicated in the lower right of each frame. For each sequence, the first two frames represent single labeling and the third frame shows double labeling. Insets denote a higher magnification of areas in dotted white boxes. Arrows in A–C denote examples of colabeling of ACF7 and CLIP170 at growing (+) ends of MTs. Arrows in D–F denote cell borders, labeled with anti-ACF7, but not antitubulin. Bar, 10 μm.

lengths of the tips of MTs that were labeled with anti-ACF7 did not appear to be significantly affected by taxol treatment. However, both the cytoskeleton and ACF7 retracted from the membrane borders of all taxol-treated cells (dotted white lines denote cell border). This was also evidenced by double label staining with anti-actin (I). After an hour of taxol treatment, MTs were short and peripheral (J–L). At this time, MT-associated anti-ACF7 staining was dramatically diminished (J).

Taxol acts specifically at the growing ends of MTs, with relative impotence at the minus ends. It acts by stabilizing the growing and shortening dynamics of the network (Derry et al., 1998). It is interesting and may be relevant that taxol dissociates CLIP170 from the growing ends of MTs, although in this case, association was lost after only 5 min of treatment (Perez et al., 1999). We speculate that similar to CLIP170, ACF7 localization may depend upon MT dynamics, and that altering the growth by taxol may influence the binding of ACF7 to plus ends. Further experiments will be necessary to assess the extent to which this notion may be correct.

Redistribution of ACF7 upon Calcium-induced Intercellular Adhesion in Keratinocytes

Kakapo null flies display a disruption in intercellular adhesion, leading to wing blisters and defects in epidermal–muscle adhesion (Gregory and Brown, 1998). To assess

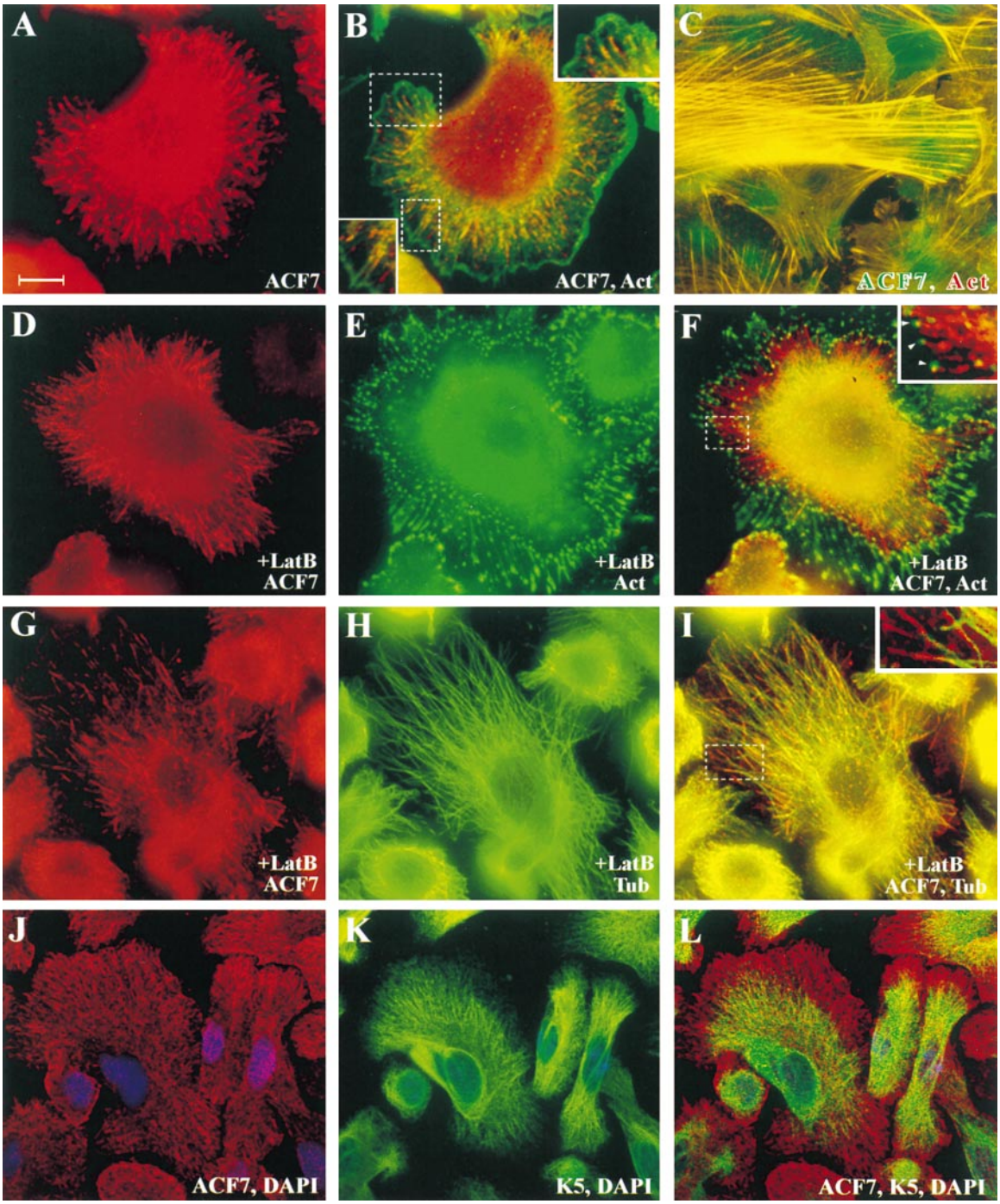

Figure 7. ACF7 associates with, but is not dependent on, the actin cytoskeleton, nor does it appear to colocalize with IFs. Keratinocytes were cultured in low calcium medium and, where indicated, were treated with 1 μg/ml latrunculin B for 30 min (+LatB) before processing for immunofluorescence microscopy. Antibodies used are indicated in lower right of each frame. Except where indicated by red/green lettering, anti-ACF7 (red); anti–α-tubulin (Tub, green); anti-actin (Act, green); antikeratin 5 (K5, green); and DAPI (blue). Arrowheads in F (inset) denote dots of actin at tips of ACF7-labeled filaments. Insets are a higher magnification of regions within dotted white boxes. Images in C and J–L were made by confocal microscopy; all others were made with conventional microscopy. Bar, 10 μm.

whether ACF7 is associated with intercellular junctions, we examined its localization after activating junction formation by calcium. 4 h of incubation in high calcium medium resulted in changes in ACF7 distribution that were accompanied by corresponding changes in organization (Fig. 9). At the colony periphery where no intercellular junctions were formed, ACF7 was still concentrated at the tips of radial MTs (A and B). At sites of intercellular adhesion, however, ACF7 localized along a line of MTs arranged parallel to and underneath the zone of adhesion (C and D, arrows). After 6 h of calcium treatment, intercellular junctions were more prevalent; colabeling with antibodies to E-cadherin or to desmoplakin revealed similar patterns with anti-ACF7 (E–H). However, in some re-

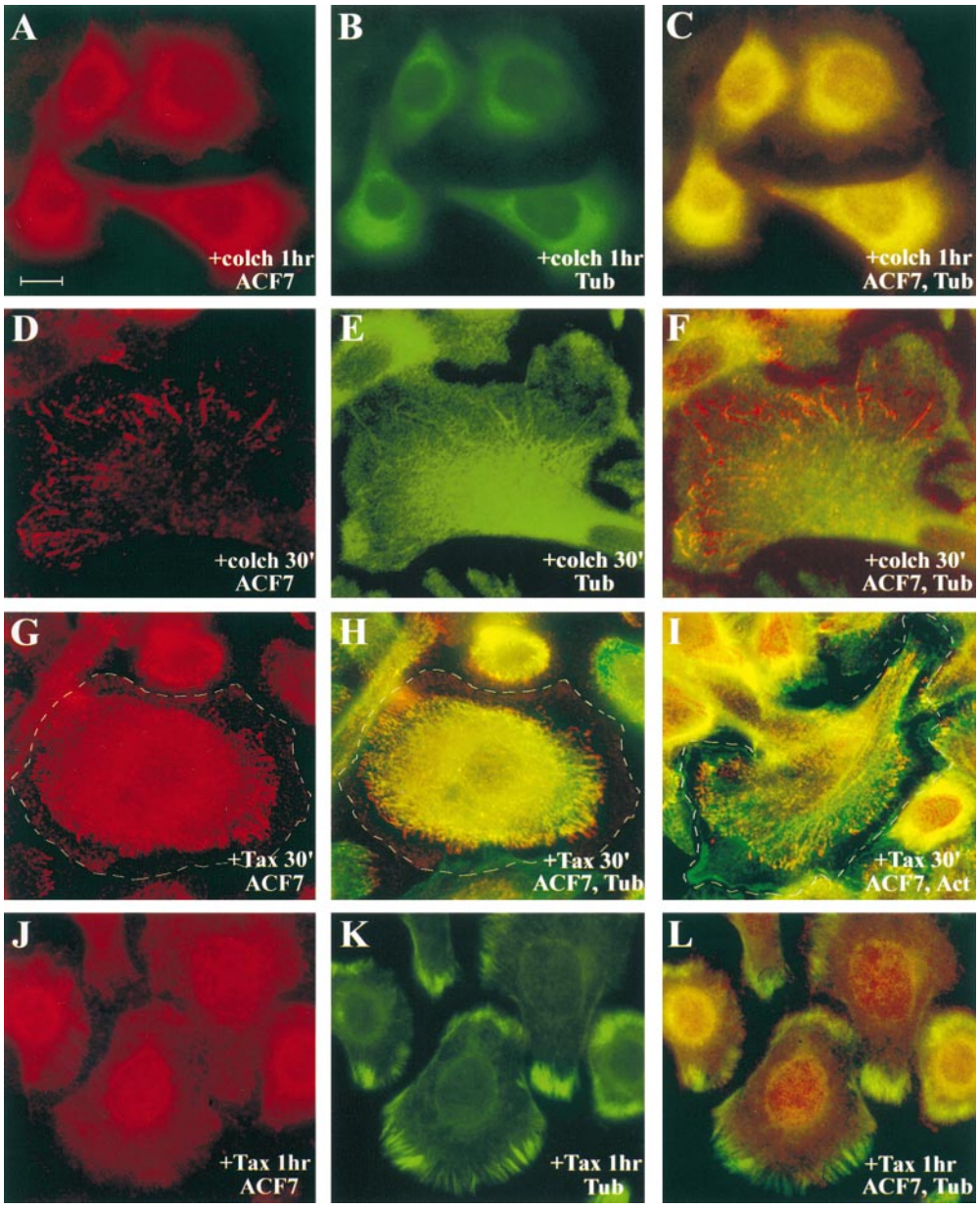

Figure 8. ACF7 localization is dependent upon the network in keratinocytes. Keratinocytes were cultured in low calcium medium and, where indicated, were treated with 1 μm colchicine (+colch) or 10 μm taxol (+Tax) for the times indicated. Immediately after treatment, cells were processed for immunofluorescence microscopy. Antibodies used are indicated the in lower right of each frame: ACF7 (red), Tub (green), and Act (green). Dotted lines in G–I denote cell border; at short times after taxol treatment, the cytoskeleton has retracted from the cell borders. Note that after 1 h of taxol treatment, ACF7 staining is lost from the MTs, which are now very short and only at the cell periphery. Bar, 10 μm.

gions, ACF7 and intercellular junction protein patterns were clearly distinct (E and F, arrows; F and H, insets).

To determine whether ACF7 is a structural part of cell–cell junctions, we explored the kinetics of adherens junction and desmosome assembly, relative to ACF7 localization. This time, nearly confluent keratinocytes were switched to high calcium medium, and cells were examined periodically within the first 2 h after the switch. In low calcium, neither E-cadherin nor desmoplakin localized to the membranes, and ACF7 localization was completely distinct (Fig. 10, A–D). The separate patterns of anti-ACF7 and anti-desmoplakin further demonstrated the specificity of these two plakin antibodies. Within an hour after inducing intercellular adhesion formation, both E-cadherin and desmoplakin began to localize to sites of intercellular contact (E–H). Despite the dynamic reorganization of these cell junction markers at these early times, ACF7 was still largely cytoskeletal and/or cytoplasmic, although some punctate staining extending out to the periphery was observed.

By 2 h, ACF7 and E-cadherin or desmoplakin patterns had merged considerably (I–L). This said, the labeling patterns still remained distinct. Thus, ACF7's localization to sites of intercellular adhesion displayed distinct kinetics relative to that of either adherens junction or desmosomal proteins, indicating that despite its association with cell–cell borders, ACF7 does not appear to be an integral component of either of these junctions. Moreover, when taken together with the anti-tubulin/anti-ACF7 staining data from Fig. 9, the data suggest that calcium stimulates a dynamic reorganization of ACF7 and the network, which is influenced by intercellular adhesion. Whether this change is dependent upon the putative calcium-binding EF-hand domain within ACF7 is an interesting question, which is beyond the scope of the present study.

As a final test, we examined whether localization of

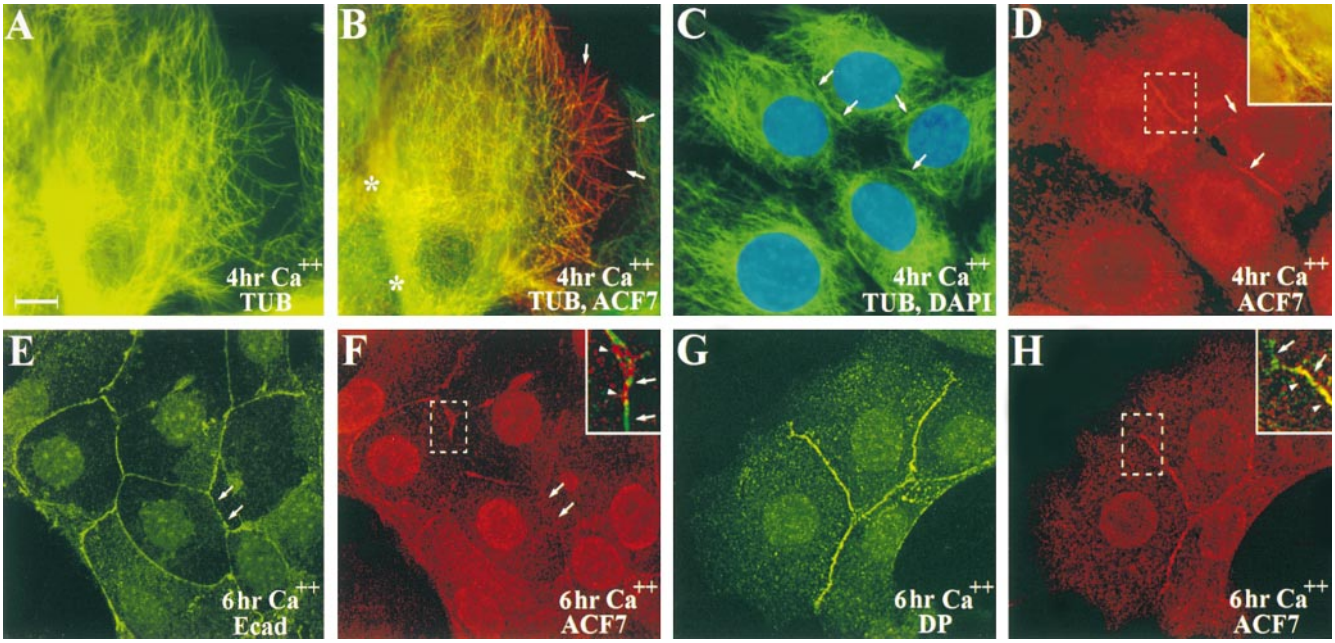

Figure 9. ACF7 reorganizes in keratinocytes after calcium is added to promote intercellular adhesion. Keratinocytes were switched from low to high calcium medium to induce adherens junction and desmosome formation, followed by processing for immunofluorescence microscopy at times indicated. Antibodies used are indicated: anti-ACF7 (red); anti–α-tubulin (TUB, green); anti–E-cadherin (Ecad, green); antidesmoplakin (DP, green); or DAPI (blue). Each pair of frames shows the same cell. Arrows in B denote ACF7 concentrated at the side of a spread cell, which is very different from that side that has close neighbors (B, asterisks). Arrows in E and F and in F and H (insets) denote regions of clear divergence in staining patterns. Arrowheads in F (inset) denote distinct ACF7 labeling; arrowheads in H (inset) denote colocalization of the label. E–H images were taken by confocal microscopy. Bar, 10 μm.

ACF7 at cell–cell borders is dependent upon MTs. To assess this possibility, we treated with colchicine simultaneously with a high calcium switch. 6 h later, it was clear that despite the disappearance of MTs, ACF7 still localized to cell–cell borders, as did markers for adherens junctions and desmosomes (data not shown). While there were fewer ACF7 labeled cell–cell junctions in the presence of colchicine, ACF7 localized to cell-cell borders independently of MTs, a feature somewhat surprising since ACF7 seemed to reorganize with MTs when cell–cell junctions were stimulated. This underscores further the complexity of ACF7's distribution and dynamics in keratinocytes.

Discussion

Fly Kakapo and Mouse ACF7: Close Cousins Not only by Sequence but also by Function

The cloning of *Drosophila* kakapo provided the first insights into the existence and function of plakins in lower eukaryotic organisms (Gregory and Brown, 1998). *Kakapo* mutants were identified in a genetic screen for flies defective in PS integrin-mediated cell–substratum adhesion. The flies displayed wing blisters because the mutant epidermal cells failed to adhere to the opposing layer of wild-type cells in the wing bilayer. This led to the significance of kakapo's Maori name, based upon a poorly flying New Zealand parrot.

Kakapo is expressed in fly epidermal cells that attach to underlying muscle through PS integrin junctions called hemiadherens junctions (Gregory and Brown, 1998; Prokop et al., 1998). The closest parallel between hemiadherens junctions in *Drosophila* and intercellular and cell–substratum junctions of mammalian epidermis has been proposed to be hemidesmosomes, which have at their core the integrin α6β4 and which bind selectively to the keratin IF network. Hemidesmosomes bind two IF-anchoring plakins, plectin and BPAG1e, and when absent, epidermal rupturing occurs (Guo et al., 1995; Andra et al., 1998).

Fly epidermal cells lack keratin IFs, and appear to utilize MTs instead for the bulk of their mechanical integrity, including that provided by cytoskeletal attachment to PS integrins (Gregory and Brown, 1998; Prokop et al., 1998). This led to the postulate that kakapo might link actin and MT cytoskeletons to the PS integrin-mediated adhesion junctions (Gregory and Brown, 1998). This said, kakapo is found at both basal and apical surfaces of the epidermal cells, in contrast to PS integrins, which are restricted to the basal surface of fly epidermis (Leptin et al., 1989). In this regard, it would seem that kakapo's functions extend beyond those of anchoring the cytoskeleton to PS integrins.

In our study, we focused on a mammalian cousin of kakapo that is more highly related to it than BPAG1e or plectin. This enabled us to test some of the hypotheses derived from the *kakapo* mutant phenotype in flies. We now provide direct evidence that ACF7 is an MT-binding protein, unveiling insights into why *kakapo* mutants cause ultrastructural perturbations in cytoskeletal networks of fly epidermal muscle attachment cells (Prokop et al., 1998).

Our discovery of a closely related kakapo cousin in mammalian epidermal cells makes it unlikely that the original comparisons drawn between hemiadherens junctions

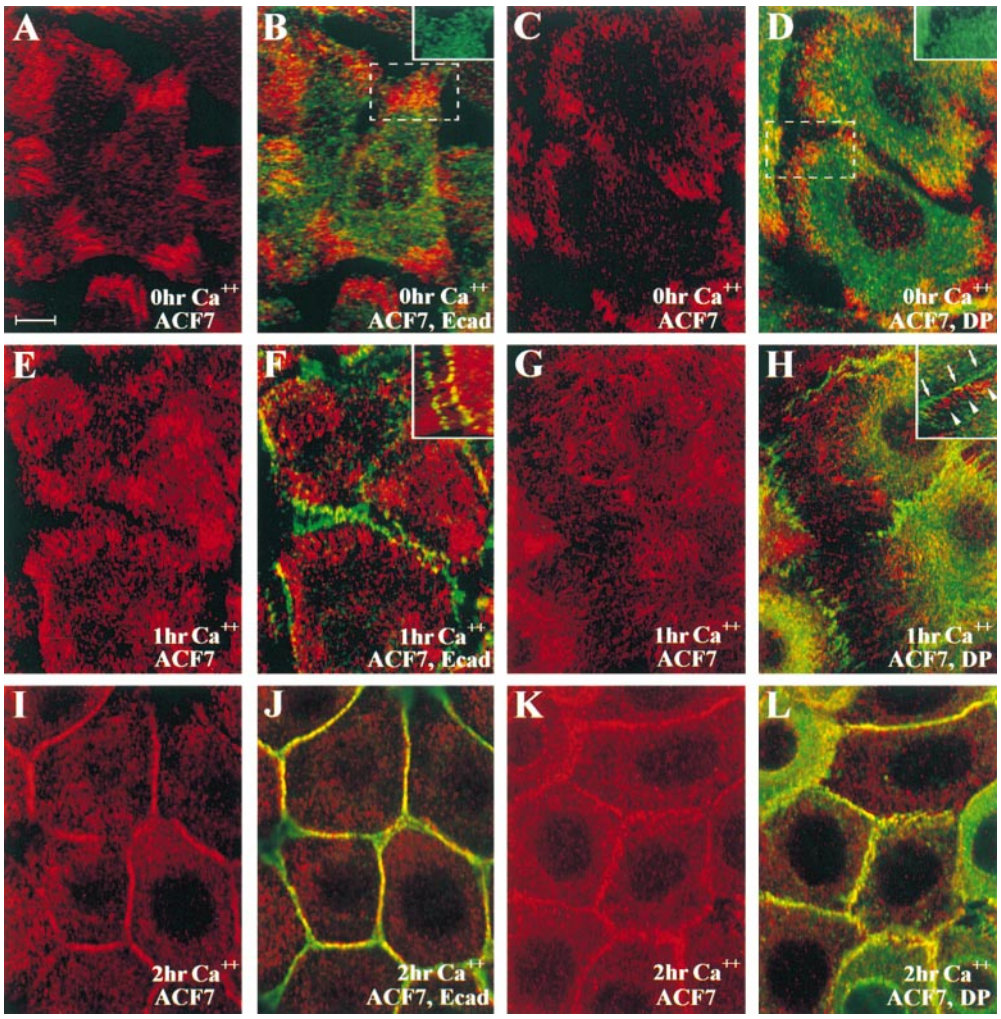

Figure 10. Membrane localization of cadherins and desmoplakin precedes ACF7 localization at sites of intercellular contact. Keratinocytes were cultured until nearly confluent, and were switched from low to high calcium to induce adherens junction and desmosome formation. Cells were processed for immunofluorescence microscopy after an additional t = 0 h (A–D), 1 h (E–H) or 2 h (I–L). Antibodies used are indicated in lower right of each frame: ACF7 (red), Ecad (green), and DP (green). For each sequence, the first frame and inset to the second frame represent single labeling, whereas the second frame shows double labeling. The insets in B and D correspond to the areas in the white dotted boxes; they are single-labeled green to show lack of specific cell–cell border staining by either Ecad or DP at t = 0. Opposing arrows/arrowheads in H (inset) denote distinct labeling patterns. All frames are confocal images. Bar, 10 μm.

and hemidesmosomes are correct. What is the function(s) of kakapo in mammalian epidermal cells and where is it involved? While unequivocal assessment of function awaits gene targeting approaches, it was intriguing to find that ACF7 localizes to the plus ends of a subset of MTs that associate with focal adhesion contacts. In epidermal keratinocytes, focal adhesion contacts are composed largely of α3β1 integrins (Jones et al., 1995), and interestingly, PS integrins are more similar in sequence to the α-β1 integrins of mammalian cells than they are to α6β4 integrins. Additionally, relevant is the recent finding that mammalian focal adhesion contacts associate with MTs as well as to the actin cytoskeleton (Kaverina et al., 1998), in contrast to hemidesmosomes, which seem to be restricted to keratin IFs in their cytoskeletal attachments (Sonnenberg et al., 1999). Taken together, our findings suggest that in mammalian epidermal cells, ACF7 functions in a fashion that is in fact similar to the role hypothesized for kakapo based upon its mutant phenotype in flies.

At mammalian focal adhesions, MTs appear to be connected after integrin clustering and attachment of actin cytoskeleton (Kaverina et al., 1998). This led to the postulate that AFs at mammalian focal adhesions might tether approaching MTs, thereby orienting their growth and stabilizing them (Cook et al., 1998). Given that ACF7 has a functional ABD, but seems to predominantly associate with radial ends of MTs, our findings raise the possibility that perhaps these MTs carry their own actin-tethering ability to focal adhesions rather than the reverse. This process could be regulated in a dynamic way, particularly if binding of ACF7 to MTs is necessary to unmask its actin binding domain. Future studies will be necessary to assess the extent to which this provocative notion might be correct.

Our results raise the possibility that ACF7 may function in part by mediating the organization of the MT cytoskeleton through its ability to make connections with the actin cytoskeleton. Connections between MTs and actin have long been postulated (Vasiliev and Gelfand, 1976; Bershadsky et al., 1978; Waterman-Storer and Salmon, 1997), but ACF7 is the first broadly expressed protein with the demonstrated ability to bind to both networks. In addition, ACF7 seems to possess the ability to selectively restrict these interactions, since only a small fraction of the actin and MT networks displayed ACF7 decoration. While this included the AFs and MTs associated with focal contacts, ACF7's connections to the cytoskeleton clearly extended beyond these interactions. In this regard, ACF7's broader localization was reminiscent of kakapo's localization to both basal and apical surfaces of epidermal cells, despite restriction of PS integrins to basal surfaces (Leptin et al., 1989).

Intercellular Adhesion and ACF7 in Keratinocytes

In *Drosophila kakapo* mutants, ruptures occurred within zones of developing epidermis that could not be explained by perturbations in PS integrin adhesion alone, leading Gregory and Brown (1998) to surmise that Kakapo function might, therefore, involve other types of cell adhesion molecules. In support of this notion, our studies reveal that a dynamic reorganization of ACF7 occurs following calcium-induced activation of intercellular adhesion. While we do not yet know the precise mechanism(s) underlying this phenomenon, it is well established that, upon calcium activation, β1 integrin expression is downregulated and integrins are lost from the surface of the keratinocyte (Hodivala and Watt, 1994). Given the associations of kakapo and ACF7 with focal adhesions, it is worth considering whether this change in integrins might trigger the redistribution of ACF7 and MTs. Perhaps a release of ACF7 from one area of the cell might mobilize it for use elsewhere.

Integrin changes upon calcium activation seem integrally linked to increases in adherens junction formation (Hodivala and Watt, 1994; Huttenlocher et al., 1998). In this regard, it was intriguing that a loss of ACF7 localization at what appeared to be focal contacts was accompanied by a new distribution of ACF7 along zones of intercellular adhesion in keratinocytes. This dynamic redistribution of ACF7, accompanied by reorientation, occurred with kinetics that were markedly distinct from those of known adherens junction and desmosomal proteins, and was independent of MT-depolymerizing agents. A priori, it is possible that ACF7 might tether MTs to adherens junctions and/or desmosomes, perhaps organizing and stabilizing MTs in a role similar to that which we postulated for ACF7 in cell–substratum associations. A multifaceted role for ACF7/kakapo in attaching and stabilizing MTs to various cellular junctions would explain why the MT network and intracellular integrity were broadly perturbed within the defective epidermal muscle attachment cells in flies (Gregory and Brown, 1998; Prokop et al., 1998; Strumpf and Volk, 1998).

ACF7: A Most Atypical Plakin

Our studies support a general model whereby ACF7 is an MT-associated protein capable of preferentially decorating the ends of MTs at the cell periphery and integrating the MTs with various cellular junctions and with the actin cytoskeleton. While the MT binding domain within the M1 domain of ACF7 is conserved among some members of the plakin family, only the sensory neural isoform 3 of BPAG1 has been previously found to bind specifically to MTs in vitro (Yang et al., 1999). In a behavior reminiscent of BPAG1n3 in cultured neurites, ACF7's cytoskeletal association was lost upon treatment of keratinocytes with MT-depolymerizing agents, and it was retained in the presence of actin-disrupting agents. However, ACF7's MT association differed from that of BPAG1 neural isoforms in several major respects. The most striking difference was that BPAG1n3 showed relatively uniform distribution across the axonal MT network, whereas ACF7 decorated only a subset of MTs, in a discontinuous fashion and with an increased level of staining towards those growing (+) ends that also associated with cellular junctions. Additionally, some neural isoforms of BPAG1 survived colchicine treatment, even though BPAG1n3 did not (Yang et al., 1999). In contrast, with the exception of cell–cell borders, the bulk of cytoskeletal-associated ACF7 in keratinocytes appeared to be dependent upon an intact MT network.

Another distinguishing feature of ACF7 is its localization to focal adhesions. Of the other known epidermal plakins, only plectin resembles ACF7 in possessing an actin binding domain (Andra et al., 1998). Intriguingly, plectin also associates with focal contacts at least in fibroblasts and glial cells (Seifert et al., 1992). However, in contrast to ACF7, plectin associates with hemidesmosomes, and it can decorate IF networks in cells. Plectin's pronounced ability to associate with IF networks through a domain (Wiche et al., 1993) that is missing in the known ACF7 isoforms may explain why the two plakins differ so markedly in some aspects of their localization.

In closing, we focused the present study on the biology of ACF7 in relation to kakapo and to other vertebrate plakins. In this regard, the regions of highest sequence similarity to plakins are those that we have analyzed, implicating ACF7 in dynamics and in connecting MTs to cellular junctions, perhaps through actin-MT cytoskeletal interactions. With a 600-kD protein, there is still much to learn about the putative interactions and biology of ACF7. We do not yet know the significance of the multiplicity of ACF7 sequences, nor do we know whether these unique amino-terminal domains might target different isoforms of ACF7 to different locales. While the presence of the EF-hand domain in the carboxy-terminal segment of ACF7 is intriguing in light of the calcium-activated redistribution of ACF7, biochemical and molecular studies will be needed to assess whether this domain plays a role in the process. Finally, it should be noted that ACF7 is really a centaurian protein in that its carboxy-terminal half resembles dystrophin more than it does a conventional plakin. What effects this may have on ACF7 function awaits further explorations into the functions and biology of this fascinating and yet Hercules-like protein.

Special thanks go to Dr. Elizabeth McNally (Department of Medicine, University of Chicago, Chicago, IL) for her helpful suggestions and advice. We thank Dr. Robert Evans (University of Colorado Health Science Center, Denver, CO) for his gift of SW13 cells. We thank Thomas Kreis' laboratory for the CLIP170 antibody, and David Lourim for assistance with protein purification.

This work was supported by a grant from the National Institutes of Health (R01-AR27883). E. Fuchs is an Investigator of the Howard Hughes Medical Institute. I. Karakesisoglou is a research associate of the HHMI.

Submitted: 19 November 1999
Revised: 21 February 2000
Accepted: 24 February 2000

References

Andra, K., H. Lassmann, R. Bittner, S. Shorny, R. Fassler, F. Propst, and G. Wiche. 1997. Targeted inactivation of plectin reveals essential function in maintaining the integrity of skin, muscle, and heart cytoarchitecture. *Genes Dev.* 11:3143–3156.

Andra, K., B. Nikolic, M. Stocher, D. Drenckhahn, and G. Wiche. 1998. Not just scaffolding: plectin regulates actin dynamics in cultured cells. *Genes Dev.* 12:3442–3451.

Bernier, G., M. Mathieu, Y. De Repentigny, S.M. Vidal, and R. Kothary. 1996. Cloning and characterization of mouse ACF7, a novel member of the dysto-

nin subfamily of actin binding proteins. *Genomics*. 39:19–29.
Bershadsky, A.D., I.S. Tint, V.I. Gelfand, V.A. Rosenblat, J.M. Vasiliev, and I.M. Gelfand. 1978. Microtubular system in cultured mouse epithelial cells. *Cell Biol. Int. Rep*. 2:345–351.
Brancolini, C., and C. Schneider. 1994. Phosphorylation of the growth arrest–specific protein Gas2 is coupled to actin rearrangements during G0→G1 transition in NIH 3T3 cells. *J. Cell Biol.* 124:743–756.
Brown, A., G. Bernier, M. Mathieu, J. Rossant, and R. Kothary. 1995. The mouse dystonia musculorum gene is a neural isoform of bullous pemphigoid antigen 1. *Nat. Genet*. 10:301–306.
Byers, T.J., A.H. Beggs, E.M. McNally, and L.M. Kunkel. 1995. Novel actin crosslinker superfamily member identified by a two step degenerate PCR procedure. *FEBS (Fed. Eur. Biochem Soc.) Lett.* 368:500–504.
Coffey, R.L., and D.L. Purich. 1995. Non-cooperative binding of the MAP-2 microtubule-binding region to microtubules. *J. Biol. Chem*. 270:1035–1040.
Cook, T.A., T. Nagasaki, and G.G. Gundersen. 1998. Rho guanosine triphosphatase mediates the selective stabilization of microtubules induced by lysophosphatidic acid. *J. Cell Biol.* 141:175–185.
Dalpe, G., N. Leclerc, A. Vallee, A. Messer, M. Mathieu, Y. De Repentigny, and R. Kothary. 1998. Dystonin is essential for maintaining neuronal cytoskeleton organization. *Mol. Cell. Neurosci*. 10:243–257.
Derry, W.B., L. Wilson, and M.A. Jordan. 1998. Low potency of taxol at microtubule minus ends: implications for its antimitotic and therapeutic mechanism. *Cancer Res.* 58:1177–1184.
Elliott, C.E., B. Becker, S. Oehler, M.J. Castanon, R. Hauptmann, and G. Wiche. 1997. Plectin transcript diversity: identification and tissue distribution of variants with distinct first coding exons and rodless isoforms. *Genomics*. 42:115–125.
Ervasti, J.M., and K.P. Campbell. 1991. Membrane organization of the dystrophin-glycoprotein complex. *Cell*. 66:1121–1131.
Fuchs, E., and Y. Yang. 1999. Crossroads on cytoskeletal highways. *Cell*. 98: 547–550.
Fuchs, E., and D. Cleveland. 1998. A structural scaffolding of intermediate filaments in health and disease. *Science*. 279:514–519.
Gallicano, I.G., P. Kouklis, C. Bauer, M. Yin, V. Vasioukhin, L. Degenstein, and E. Fuchs. 1998. Desmoplakin is required early in development for assembly of desmosomes and cytoskeletal linkage. *J. Cell Biol.* 143:2009–2022.
Gregory, S.L., and N.H. Brown. 1998. *kakapo*, a gene required for adhesion between and within cell layers in *Drosophila*, encodes a large cytoskeletal linker protein related to plectin and dystrophin. *J. Cell Biol.* 143:1271–1282.
Guo, L., L. Degenstein, J. Dowling, Q.-C. Yu, R. Wollmann, B. Perman, and E. Fuchs. 1995. Gene targeting of BPAG1: abnormalities in mechanical strength and cell migration in stratified squamous epithelia and severe neurologic degeneration. *Cell*. 81:233–243.
Hodivala, K.J., and F.M. Watt. 1994. Evidence that cadherins play a role in the downregulation of integrin expression that occurs during keratinocyte terminal differentiation. *J. Cell Biol.* 124:589–600.
Huttenlocher, A., M. Lakonishok, M. Kinder, S. Wu, T. Truong, K.A. Knudsen, and A.F. Horwitz. 1998. Integrin and cadherin synergy regulates contact inhibition of migration and motile activity. *J. Cell Biol.* 141:515–526.
Ikura, M. 1996. Calcium binding and conformational response in EF-hand proteins. *Trends. Biochem. Sci.* 21:14–17.
Jones, P.H., S. Harper, and F.M. Watt. 1995. Stem cell patterning and fate in human epidermis. *Cell*. 80:83–93.
Jongstra-Bilen, J., P.A. Janmey, J.H. Hartwig, S. Galea, and J. Jongstra. 1992. The lymphocyte-specific protein LSP1 binds to F-actin and to the cytoskeleton through its COOH-terminal basic domain. *J. Cell Biol.* 118:1443–1453.
Kaverina, I., K. Rottner, and J.V. Small. 1998. Targeting, capture, and stabilization of microtubules at early focal adhesions. *J. Cell Biol.* 142:181–190.
Kawasaki, H., and R.H. Kretsinger. 1995. Calcium-binding proteins 1: EF-hands. *Protein Profile*. 2:297–490.
Koenig, M., and L.M. Kunkel. 1990. Detailed analysis of the repeat domain of dystrophin reveals four potential hinge segments that may confer flexibility. *J. Biol. Chem*. 265:4560–4566.
Kouklis, P., E. Hutton, and E. Fuchs. 1994. Making the connection: keratin intermediate filaments and desmosomes proteins. *J. Cell Biol.* 127:1049–1060.
Kowalczyk, A.P., E.A. Bornslaeger, J.E. Borgwardt, H.L. Palka, A.S. Dhaliwal, C.M. Corcoran, M.F. Denning, and K.J. Green. 1997. The amino-terminal domain of desmoplakin binds to plakoglobin and clusters desmosomal cadherin–plakoglobin complexes. *J. Cell Biol.* 139:773–784.
Kowalczyk, A.P., E.A. Bornslaeger, S.M. Norvell, H.L. Palka, and K.J. Green. 1999. Desmosomes: intercellular adhesive junctions specialized for attachment of intermediate filaments. *Int. Rev. Cytol.* 185:237–302.
Leptin, M., T. Bogaert, R. Lehmann, and M. Wilcox. 1989. The function of PS integrins during *Drosophila* embryogenesis. *Cell*. 56:401–408.
Leung, C.L., D. Sun, and R.K.H. Liem. 1999a. The intermediate filament protein peripherin is the specific interaction partner of mouse BPAG1-n (Dystonin) in neurons. *J. Cell Biol.* 144:435–446.
Leung, C.L., D. Sun, M. Zheng, D.R. Knowles, and R.K.H. Liem. 1999b. Microtubule actin cross-linking factor (MACF): a hybrid of dystonin and dystrophin that can interact with the actin and microtubule cytoskeletons. *J. Cell Biol.* 147:1275–1287.
Lo, S.H., P.A. Janmey, J.H. Hartwig, and L.B. Chen. 1994. Interactions of tensin with actin and identification of its three distinct actin-binding domains. *J. Cell Biol.* 125:1067–1075.
Nagase, T., K. Ishikawa, M. Suyama, R. Kikuno, M. Hirosawa, N. Miyajima, A. Tanaka, H. Kotani, N. Nomura, and O. Ohara. 1998. Prediction of the coding sequences of unidentified human genes. XII. The complete sequences of 100 new cDNA clones from brain which code for large proteins in vitro. *DNA Res.* 5:355–364.
O'Keefe, E.J., R.A. Briggaman, and B. Herman. 1987. Calcium-induced assembly of adherens junctions in keratinocytes. *J. Cell Biol.* 105:807–817.
Okuda, T., S. Matsuda, S. Nakatsugawa, Y. Ichigotani, N. Iwahashi, M. Takahashi, T. Ishigaki, and M. Hamaguchi. 1999. Molecular cloning of macrophin, a human homologue of *Drosophila* kakapo with a close structural similarity to plectin and dystrophin. *Biochem. Biophys. Res. Commun*. 264: 568–574.
Pasdar, M., Z. Li, and K.A. Krzeminski. 1992. Desmosome assembly in MDCK epithelial cells does not require the presence of functional microtubules. *Cell Motil. Cytoskeleton*. 23:201–212.
Perez, F., G.S. Diamantopoulos, R. Stalder, and T.E. Kreis. 1999. CLIP-170 highlights growing microtubule ends in vivo. *Cell*. 96:517–527.
Prokop, A., J. Uhler, J. Roote, and M. Bate. 1998. The kakapo mutation affects terminal arborization and central dendritic sprouting of *Drosophila* motorneurons. *J. Cell Biol.* 143:1283–1294.
Rezniczek, G.A., J.M. de Pereda, S. Reipert, and G. Wiche. 1998. Linking integrin α6β4-based cell adhesion to the intermediate filament cytoskeleton: direct interaction between the β4 subunit and plectin at multiple molecular sites. *J. Cell Biol.* 141:209–225.
Ruhrberg, C., and F.M. Watt. 1997. The plakin family: versatile organizers of cytoskeletal architecture. *Curr. Opin. Genet. Dev*. 7:392–397.
Ruhrberg, C., J.A. Williamson, A. Maatta, and F.M. Watt. 1998. The periplakin gene maps to 16p13.3 in human and 16A-B1 in mouse. *Genomics*. 49:157–159.
Schaapveld, R.Q., L. Borradori, D. Geerts, M.R. van Leusden, I. Kuikman, M.G. Nievers, C.M. Niessen, R.D. Steenbergen, P.J. Snijders, and A. Sonnenberg. 1998. Hemidesmosome formation is initiated by the β4 integrin subunit, requires complex formation of β4 and HD1/plectin, and involves a direct interaction between β4 and the bullous pemphigoid antigen 180. *J. Cell Biol.* 142:271–284.
Schneider, C., R.M. King, and L. Philipson. 1988. Genes specifically expressed at growth arrest of mammalian cells. *Cell*. 54:787–793.
Seifert, G.J., D. Lawson, and G. Wiche. 1992. Immunolocalization of the intermediate filament-associated protein plectin at focal contacts and actin stress fibers. *Eur. J. Cell Biol.* 59:138–147.
Smith, E., and E. Fuchs. 1998. Defining desmoplakin's interactions with desmosomes. *J. Cell Biol.* 141:1229–1241.
Sonnenberg, A., M. Nievers, R. Schaapveld, D. Geerts, C. Niessen, and L. Borradori. 1999. Interaction of BP180 and alpha6beta4. *J. Invest. Dermatol.* 112: 830–832.
Stappenbeck, T.S., and K.J. Green. 1992. The desmoplakin carboxyl terminus coaligns with and specifically disrupts intermediate filament networks when expressed in cultured cells. *J. Cell Biol.* 116:1197–1209.
Straub, V., and K.P. Campbell. 1997. Muscular dystrophies and the dystrophin-glycoprotein complex. *Curr. Opin. Neurol.* 10:168–175.
Strumpf, D., and T. Volk. 1998. Kakapo, a novel cytoskeletal-associated protein is essential for the restricted localization of the neuregulin-like factor, vein, at the muscle-tendon junction site. *J. Cell Biol.* 143:1259–1270.
Sun, Y., J. Zhang, S.K. Kraeft, D. Auclair, M.S. Chang, Y. Liu, R. Sutherland, R. Salgia, J.D. Griffin, L.H. Ferland, and L.B. Chen. 1999. Molecular cloning and characterization of human trabeculin-alpha, a giant protein defining a new family of actin-binding proteins. *J. Biol. Chem*. 274:33522–33530.
Svitkina, T., A. Verkhovsky, and G. Borisy. 1996. Plectin sidearms mediate interaction of intermediate filaments with microtubules and other components of the cytoskeleton. *J. Cell Biol.* 135:991–1007.
Togel, M., G. Wiche, and F. Propst. 1998. Novel features of the light chain of microtubule-associated protein MAP1B: microtubule stabilization, self interaction, actin filament binding, and regulation by the heavy chain. *J. Cell Biol*. 143:695–707.
Vasiliev, J.M., and I.M. Gelfand. 1976. Morphogenetic reactions and locomotory behavior of transformed cells in culture. *Fundam. Asp. Metastasis.* 71–98.
Wallis, K.T., S. Azhar, M.B. Rho, S.A. Lewis, N.J. Cowan, and D.B. Murphy. 1993. The mechanism of equilibrium binding of microtubule-associated protein 2 to microtubules. Binding is a multi-phasic process and exhibits positive cooperativity. *J. Biol. Chem*. 268:15158–15167.
Waterman-Storer, C.M., and E.D. Salmon. 1997. Actomyosin-based retrograde flow of microtubules in the lamella of migrating epithelial cells influences microtubule dynamic instability and turnover and is associated with microtubule breakage and treadmilling. *J. Cell Biol*. 139:417–434.
Watt, F.M., D.L. Mattey, and D.R. Garrod. 1984. Calcium-induced reorganization of desmosomal components in cultured human keratinocytes. *J. Cell Biol.* 99:2211–2215.
Wiche, G., D. Gromov, A. Donovan, M.J. Castanon, and E. Fuchs. 1993. Expression of plectin mutant cDNA in cultured cells indicates a role of COOH-terminal domain in intermediate filament association. *J. Cell Biol.* 121:607–619.
Yang, Y., J. Dowling, Q.-C. Yu, P. Kouklis, D.W. Cleveland, and E. Fuchs. 1996. An essential cytoskeletal linker protein connecting actin microfilaments to intermediate filaments. *Cell*. 86:655–665.
Yang, Y., C. Bauer, G. Strasser, R. Wollman, J.P. Julien, and E. Fuchs. 1999. Integrators of the cytoskeleton which stabilize microtubules. *Cell*. 98:229–238.